



## Air quality improvement in a megacity: implications from 2015 Beijing Parade Blue pollution control actions

Wen Xu<sup>1,a,\*</sup>, Wei Song<sup>2,\*</sup>, Yangyang Zhang<sup>1,\*</sup>, Xuejun Liu<sup>1</sup>, Lin Zhang<sup>3</sup>, Yuanhong Zhao<sup>3</sup>, Duanyang Liu<sup>4</sup>, Aohan Tang<sup>1</sup>, Daowei Yang<sup>1</sup>, Dandan Wang<sup>1</sup>, Zhang Wen<sup>1</sup>, Yuepeng Pan<sup>5</sup>, David Fowler<sup>6</sup>, Jeffrey L. Collett Jr.<sup>7</sup>, Jan Willem Erisman<sup>8</sup>, Keith Goulding<sup>9</sup>, Yi Li<sup>10</sup>, and Fusuo Zhang<sup>1</sup>

<sup>1</sup>College of Resources and Environmental Sciences, Center for Resources, Environment and Food Security, Key Laboratory of Plant–Soil Interactions of MOE, China Agricultural University, Beijing, 100193, China

<sup>2</sup>Institute of Surface–Earth System Science, Tianjin University, Tianjin, 300072, China

<sup>3</sup>Laboratory for Climate and Ocean–Atmosphere Studies, Department of Atmospheric and Oceanic Sciences, School of Physics, Peking University, Beijing, 100871, China

<sup>4</sup>Jiangsu Meteorological Observatory, Nanjing, 210008, China

<sup>5</sup>State Key Laboratory of Atmospheric Boundary Layer Physics and Atmospheric Chemistry (LAPC), Institute of Atmospheric Physics, Chinese Academy of Sciences, Beijing, 100029, China

<sup>6</sup>Centre for Ecology and Hydrology Edinburgh, Bush Estate, Penicuik, Midlothian, EH26 0QB, UK

<sup>7</sup>Department of Atmospheric Science, Colorado State University, Fort Collins, CO 80523, USA

<sup>8</sup>Louis Bolk Institute, Hoofdstraat 24, 3972 LA Driebergen, the Netherlands

<sup>9</sup>The Sustainable Soil and Grassland Systems Department, Rothamsted Research, West Common, Harpenden, Hertfordshire, AL5 2JQ, UK

<sup>10</sup>Arizona Department of Environmental Quality, Phoenix, AZ 85007, USA

<sup>a</sup>current address: State Key Laboratory of Urban and Regional Ecology, Research Center for Eco-Environmental Sciences, Chinese Academy of Sciences, Shuangqing Road 18, Haidian District, Beijing, 100085, China

\*These authors contributed equally to this work.

Correspondence to: Xuejun Liu (liu310@cau.edu.cn)

Received: 6 July 2016 – Published in Atmos. Chem. Phys. Discuss.: 5 September 2016

Revised: 12 December 2016 – Accepted: 12 December 2016 – Published: 2 January 2017

**Abstract.** The implementation of strict emission control measures in Beijing and surrounding regions during the 2015 China Victory Day Parade provided a valuable opportunity to investigate related air quality improvements in a megacity. We measured NH<sub>3</sub>, NO<sub>2</sub> and PM<sub>2.5</sub> at multiple sites in and outside Beijing and summarized concentrations of PM<sub>2.5</sub>, PM<sub>10</sub>, NO<sub>2</sub>, SO<sub>2</sub> and CO in 291 cities across China from a national urban air quality monitoring network between August and September 2015. Consistently significant reductions of 12–35 % for NH<sub>3</sub> and 33–59 % for NO<sub>2</sub> in different areas of Beijing during the emission control period (referred to as the Parade Blue period) were observed compared with measurements in the pre- and post-Parade Blue periods without emission controls. Average NH<sub>3</sub> and NO<sub>2</sub> concentrations at sites near traffic were strongly correlated and

showed positive and significant responses to traffic reduction measures, suggesting that traffic is an important source of both NH<sub>3</sub> and NO<sub>x</sub> in urban Beijing. Daily concentrations of PM<sub>2.5</sub> and secondary inorganic aerosol (sulfate, ammonium and nitrate) at the urban and rural sites both decreased during the Parade Blue period. During (after) the emission control period, concentrations of PM<sub>2.5</sub>, PM<sub>10</sub>, NO<sub>2</sub>, SO<sub>2</sub> and CO from the national city-monitoring network showed the largest decrease (increase) of 34–72 % (50–214 %) in Beijing, a smaller decrease (a moderate increase) of 1–32 % (16–44 %) in emission control regions outside Beijing and an increase (decrease) of 6–16 % (–2–7 %) in non-emission-control regions of China. Integrated analysis of modelling and monitoring results demonstrated that emission control measures made a major contribution to air quality improve-

ment in Beijing compared with a minor contribution from favourable meteorological conditions during the Parade Blue period. These results show that controls of secondary aerosol precursors ( $\text{NH}_3$ ,  $\text{SO}_2$  and  $\text{NO}_x$ ) locally and regionally are key to curbing air pollution in Beijing and probably in other mega cities worldwide.

## 1 Introduction

China's economy has made great advances over the last 3 decades. Its gross domestic production (GDP) ranked 15th in the world in 1978 but has risen to second place since 2010. During this period, environmental pollution has greatly increased, including soil, water and air pollution (Chan and Yao, 2008; Guo et al., 2010; Chen et al., 2014; Lu et al., 2015), which has become a major issue for the country. The Chinese government and people have grown particularly concerned about reducing air pollution since the large-scale haze pollution that occurred in China in January 2013. This episode affected an area of approximately 1.3 million  $\text{km}^2$  and 800 million people (Huang et al., 2014). It led to serious human health problems and forced the Chinese government to address the problem of very large exposures of the Chinese population to  $\text{PM}_{2.5}$  (particulate matter  $\leq 2.5 \mu\text{m}$  in aerodynamic diameter) pollution. For example, compared with a similar winter period without haze pollution (daily child patients  $< 600$ ), more than 7000 daily child patients were reported in Beijing Children's Hospital during the smog period in January 2013 ([http://qnck.cyol.com/html/2014-01/01/nw.D110000qnck\\_20140101\\_1-28.htm](http://qnck.cyol.com/html/2014-01/01/nw.D110000qnck_20140101_1-28.htm)). In response to this the "Atmospheric Pollution Prevention and Control Action Plan" was implemented by the Chinese government in September 2013, aiming to reduce  $\text{PM}_{2.5}$  in Beijing by at least 25 % from the 2012 level by 2017.

Many industrialized megacities have experienced severe air pollution, such as Los Angeles during the 1940s–1970s (Haagen-Smit, 1952; Parrish et al., 2011), Mexico city in the 1980s (Parrish et al., 2011) and London in the 1950s (Davis et al., 2002). In these megacities, however, enormous progress in improving air quality has been achieved with the implementation of various emission control strategies over recent decades, despite rapid population growth and urbanization. According to Parrish et al. (2011), first stage smog alerts in Los Angeles have decreased from some 200 per year in the 1970s to about 10 per year now, and concentrations of air pollutants in Mexico City have been reduced substantially over the past decades. Also, air quality is now much better in London, with mean annual  $\text{PM}_{10}$  (particulate matter  $\leq 10 \mu\text{m}$  in aerodynamic diameter) levels closer to  $30 \mu\text{g m}^{-3}$  than the  $300 \mu\text{g m}^{-3}$  50 years ago (and approx.  $3000 \mu\text{g m}^{-3}$  in December 1952) (Davis et al., 2002).

Beijing, the capital of China, is one of the largest megacities in the world with 22 million inhabitants and an area of

16 800  $\text{km}^2$ . The city is enclosed by the Yan Mountains to the north and Taihang Mountains to the west. Its fan-shaped topography permits efficient southerly transport of pollutants to Beijing, which reduces air quality (Chen et al., 2015). A 70th anniversary victory parade was held in Beijing on 3 September 2015 to commemorate the conclusion of the second Sino-Japanese War and the end of World War II. The Chinese government imposed a series of strict and urgent air pollutant emission-reduction measures to improve air quality during what has been called the "Parade Blue" period, from 20 August to 3 September 2015, in Beijing and surrounding regions (including Tianjin City, Inner Mongolia Autonomous Region, Hebei, Shandong, Shanxi and Henan provinces) to guarantee better air quality in the city. During this period, motor vehicles (except taxis and buses) with even or odd registration numbers were banned on alternate days, 1927 industrial enterprises had to limit production or were shut down and hundreds of construction sites in Beijing were closed, reducing air pollutant emissions by 40 % (<http://gongyi.sohu.com/20150826/n419765215.shtml>). For all seven of the cities, provinces and autonomous regions, air pollutant emissions during the Parade Blue period were decreased by 30 % through a variety of reduction measures (<http://news.sohu.com/20150819/n419198051.shtml>). No additional pollution control measures were taken in other regions of China (outside Beijing and surrounding regions) during this period.

Previous studies have attempted to quantify the role of short-term pollutant emission control measures in air quality improvement in Beijing during the 2008 Olympics (Wang et al., 2009, 2010; Shen et al., 2011) and the 2014 Asia-Pacific Economic Cooperation (APEC) meeting (Chen et al., 2015). In addition, Tang et al. (2015) reported that local emissions are the key factors determining the formation and development of air pollution in the Beijing area. Ianniello et al. (2010) inferred that traffic may be an important emission source of  $\text{NH}_3$  in Beijing. However, the above studies did not systematically answer the two following questions: what were (1) the contribution of ammonia ( $\text{NH}_3$ ) sources to urban  $\text{PM}_{2.5}$  pollution and (2) the relative roles of pollution control measures and weather conditions in air quality improvement? The present study attempts to examine these important topics by taking advantage of the implementation of emission controls for the 70th anniversary victory parade. We present results showing changes in concentrations of atmospheric pollutants (i.e.  $\text{NH}_3$ ,  $\text{NO}_2$ ,  $\text{PM}_{2.5}$  and associated inorganic water-soluble ions, or WSIs) before, during and after the Parade Blue period, obtained from in situ measurements at 31 sites in and outside Beijing. In addition, we compare the Chinese Ministry of Environmental Protection officially released daily concentrations of  $\text{PM}_{2.5}$ ,  $\text{PM}_{10}$ ,  $\text{NO}_2$ ,  $\text{SO}_2$  and CO at 291 cities in China during the same period. The first results from the analysis of this extensive dataset reveal clear effects of the Parade Blue emission reduction measures on air quality improvement and provide a scientific basis for

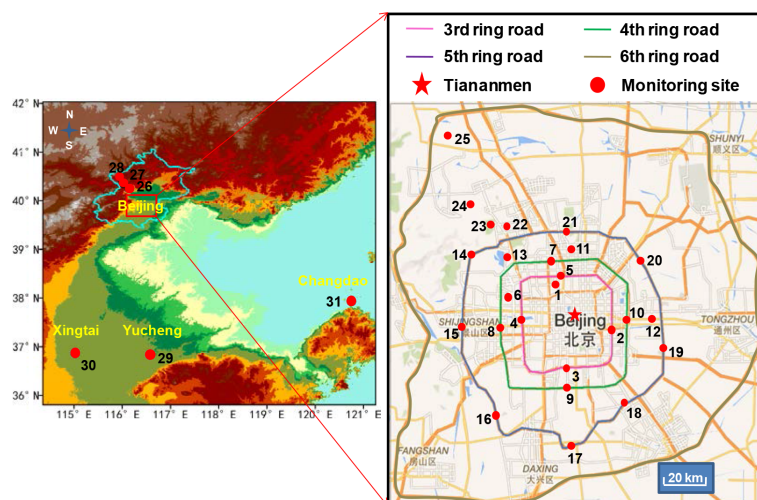


**Figure 1.** Maps showing the 31 monitoring sites, the Beijing municipality (the areas within the blue line) and the surrounding regions. Also shown are locations of Tiananmen and the third, fourth, fifth and sixth ring roads.

demonstrating the effectiveness of such control measures for air pollution in mega cities.

## 2 Materials and methods

### 2.1 Site selection and description

Thirty-one air pollution monitoring sites have been established in and outside Beijing municipality, with longitudes ranging from 115.02 to 118.20° E and latitudes from 36.84 to 40.34° N (Fig. 1). The 28 monitoring sites in Beijing municipality are grouped into road and non-road sites to better distinguish the impacts of control measures on sites near traffic. A brief description of all the sites is given below. Detailed information, including specific sampling site, site type and potential emission sources for each site, is listed in Table S1 in the Supplement.

In Beijing, 16 roadside monitoring sites are homogeneously distributed at the edges of three major roads, including four sites each on the third and fourth ring roads, and eight sites on the fifth ring road. Additional road sites (sites 26 to 28) are in northwestern rural regions near the Yanshan mountains. Site 26 is located at the edge of the Badaling highway, about 46 km northwest of the centre of Beijing. Sites 27 and 28 are located, respectively, inside (100 m from the exit) and outside (30 m from the entrance) the Badaling Highway Tunnel (1091.2 m long), which has two traffic tunnels with one lane in each. The road sites were strongly and directly influenced by vehicle emissions. Nine non-road sites were chosen over a wide area, extending from an urban area (site 1) near the city centre, through suburban areas (sites 6, 11, 12 and 13) between the third and fifth ring roads, and ending in rural areas (sites 22 to 25) between the northwest fifth and sixth ring roads. These are likely to be

polluted by emissions from various sources, including dense housing, industry, cropland, small villages, etc.

Outside Beijing, site 29 is located in a rural area of Yucheng city, Shandong province. Site 30 is located in Quzhou county, Hebei province, which is a typical rural agricultural site with a recently constructed industrial district. Site 31 is a regional background site located in Changdao county, Shandong.

### 2.2 Sampling procedure and sample analysis

Atmospheric  $\text{NH}_3$ ,  $\text{NO}_2$  and  $\text{PM}_{2.5}$  were measured from 3 August to 30 September 2015. The period can be divided into three phases: (1) 3–19 August (named pre-Parade Blue period), (2) 20 August–3 September (Parade Blue period) and (3) 4–30 September (post-Parade Blue period). The sampling durations, measured pollutants and number of samples for all the sites during each phase are summarized in Table S1. The measurements of  $\text{NH}_3$ ,  $\text{NO}_2$  and  $\text{PM}_{2.5}$  were not concurrently made at most sites due to a shortage of manpower and samplers, but the corresponding sampling sites together covered the major emission sources of measured pollutants. Methods for sampling gases and  $\text{PM}_{2.5}$  are briefly presented below. For further details of the methodology the reader is referred to relevant previous publications (Xu et al., 2014, 2015, 2016).

Gaseous  $\text{NH}_3$  and  $\text{NO}_2$ :  $\text{NH}_3$  samples were collected using ALPHA passive samplers (adapted low-cost high absorption, provided by the Centre for Ecology and Hydrology, Edinburgh, UK) and  $\text{NO}_2$  samples using Gradko diffusion tubes (Gradko International Limited, UK). At each site, three ALPHA samplers and/or three  $\text{NO}_2$  tubes were deployed under a PVC shelter (2 m above the ground) to protect the samplers from rain and direct sunlight (pictures for four selected road sites are shown in Fig. S1 of the Supplement). The samplers

were exposed for 7 to 14 days during the three study phases.  $\text{NH}_3$  was extracted with high-purity water (18.2 M $\Omega$ ) and analysed using a continuous-flow analyzer (Seal AA3, Germany).  $\text{NO}_2$  samples, also extracted with high-purity water, were analysed using a colorimetric method by absorption at a wavelength of 542 nm. More details of the passive samplers and their laboratory preparation and analysis can be found in Xu et al. (2014, 2015).

Airborne  $\text{PM}_{2.5}$ : 24 h  $\text{PM}_{2.5}$  samples were collected on 90 mm quartz fiber filters (Whatman QM/A, Maidstone, UK) using medium-volume samplers (TH-150CIII, Tianhong Co., Wuhan, China), at a flow rate of 100 L  $\text{min}^{-1}$ . The  $\text{PM}_{2.5}$  mass was determined using the standard gravimetric method, and one quarter of each  $\text{PM}_{2.5}$  sample was ultrasonically extracted with 10 mL high-purity water for 30 min, with the extract being filtered by a syringe filter (0.45  $\mu\text{m}$ , Tengda Inc., China). The water-soluble cations ( $\text{NH}_4^+$ ,  $\text{Na}^+$ ,  $\text{Ca}^{2+}$ ,  $\text{K}^+$ ,  $\text{Mg}^{2+}$ ) and anions ( $\text{NO}_3^-$ ,  $\text{SO}_4^{2-}$ ,  $\text{F}^-$ ,  $\text{Cl}^-$ ) in the extract were analysed using Dionex-600 and Dionex-2100 Ion Chromatographs (Dionex Inc., Sunnyvale, CA, USA), respectively (Zhang et al., 2011; Tao et al., 2014).

### 2.3 Quality assurance and quality control

All samples were prepared and measured in the Key Laboratory of Plant–Soil Interactions, Chinese Ministry of Education, China Agricultural University, which has a complete and strict quality control system. Three field (travel) blanks were prepared for each batch of samples and analysed together with those samples. All reported concentrations of gases and  $\text{PM}_{2.5}$  mass and ion concentrations are corrected for the blanks. The detection limits were 0.01–0.02  $\text{mg L}^{-1}$  for the measured ions. The measurement precisions were in the range of 5–10 % for  $\text{NH}_3$ ,  $\text{NO}_2$ ,  $\text{PM}_{2.5}$  mass and WSI concentrations. Quality assurance was routinely (once every 15–20 samples) checked using standard (designed specific concentrations of various ions) samples during sample analysis.

### 2.4 Other data collection

The 24 h (daily) average concentrations of  $\text{PM}_{2.5}$ ,  $\text{PM}_{10}$ ,  $\text{NO}_2$ ,  $\text{SO}_2$  and CO measured in 291 cities across China (including Beijing, surrounding 63 cities in emission control regions (hereafter termed to emission control regions, excluding Beijing), and 227 cities in other regions of China (hereafter referred to as non-emission-control regions) during the Pre-Parade Blue, Parade Blue and post-Parade periods were downloaded from the Ministry of Environmental Protection (MEP) of China (<http://www.mep.gov.cn>). These data for each city are summarized in Tables S2–6. For Beijing, each pollutant's daily individual Air Quality Index (AQI) during the above three periods was calculated from the 24 h average concentration. The highest individual AQI was selected and used as the daily AQI. An AQI of 0–50, 51–100,

101–150 and 151–200 is classified as “excellent”, “good”, “slightly polluted” and “moderately polluted”, respectively. Details of the calculations of AQI and the associated classification of air quality are given in the Chinese Technical Regulations on AQI (MEPC, 2012).

Daily meteorological data in the above mentioned 291 cities for wind speed (WS), temperature ( $T$ ) and relative humidity (RH) during the Parade Blue period and non-Parade Blue periods (the pre- and post-Parade Blue periods) were obtained from Weather Underground (<http://www.underground.com>). The daily precipitation and half-hourly wind speed and direction were measured in Beijing. The NCEP/NCAR global reanalysis meteorological data (including daily wind speed, wind direction, sea surface pressure and precipitation) during the same periods were provided by Oceanic and Atmospheric Research/ESRL Physical Sciences Division, National Oceanic and Atmospheric Administration (NOAA), Boulder, Colorado, USA, from their website (<http://www.esrl.noaa.gov/psd>). The daily mean atmospheric mixing layer height (MLH) in Beijing during the period from 3 August to 30 September 2015 was calculated using the method described in Holzworth (1964, 1967).

### 2.5 Back trajectories and statistical analysis

The 72 h (3-day) backward trajectories arriving at Beijing were calculated four times a day (00:00, 06:00, 12:00 and 18:00 UTC) at 100 m height using the Hybrid Single Particle Lagrangian Integrated Trajectory (HYSPPLIT4) from NOAA 4.9 model (Draxler and Hess, 1997). Meteorological data with a resolution of  $0.5^\circ \times 0.5^\circ$  were input from the Global Data Assimilation System (GDAS) meteorological data archives of the Air Resource Laboratory (NOAA). The trajectories were then grouped into four clusters during each period using cluster analysis based on the total spatial variance (TSV) method (Draxler et al., 2012). Values of  $\text{NH}_3$ ,  $\text{NO}_2$ ,  $\text{PM}_{2.5}$  and ion concentrations per study phase at the sampling sites are shown as the mean  $\pm$  standard error. Temporal differences between study phases of concentrations of measured gases ( $\text{NH}_3$  and  $\text{NO}_2$ ) and the MEP of reported pollutants (i.e.  $\text{PM}_{2.5}$ ,  $\text{PM}_{10}$ ,  $\text{NO}_2$ ,  $\text{SO}_2$  and CO) were investigated using paired  $t$  tests while those of measured  $\text{PM}_{2.5}$  mass and associated ionic components were investigated using a non-parametric Mann–Whitney  $U$  test. All statistical analyses were performed using SPSS11.5 (SPSS Inc., Chicago, IL, USA). Statistically significant differences were set at  $p < 0.05$  unless otherwise stated.

## 3 Results

### 3.1 Concentrations of gaseous $\text{NH}_3$ and $\text{NO}_2$

Ambient  $\text{NH}_3$  concentrations varied greatly during the pre-Parade Blue, Parade Blue and post-Parade Blue periods, with values of 8.2–31.7, 7.8–50.7 and 7.4–40.2  $\mu\text{g m}^{-3}$ , re-

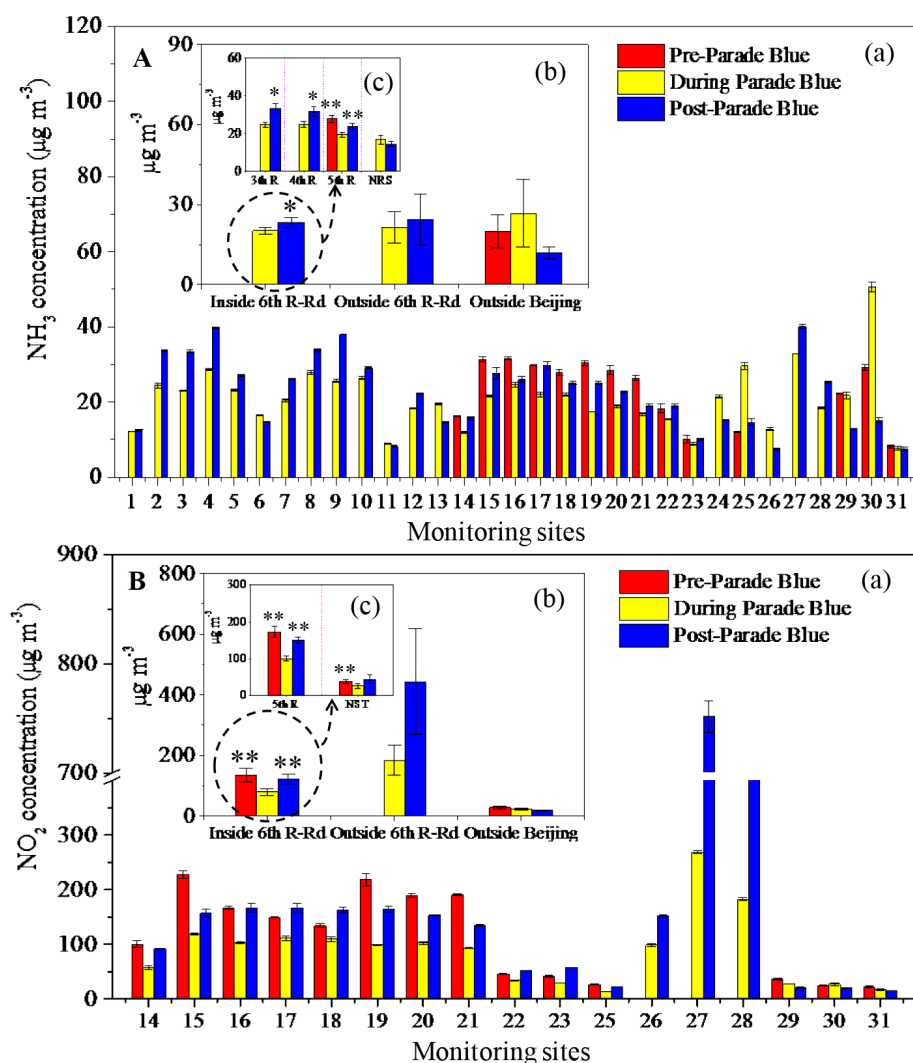


**Figure 2.** Concentrations of  $\text{NH}_3$  (A) and  $\text{NO}_2$  (B) during the monitoring periods at different observation scales: concentrations at 31 ( $\text{NH}_3$ ) or 17 ( $\text{NO}_2$ ) sites (a), averaged concentrations for the sites inside the sixth ring (R) road (Rd), outside the sixth ring (R) road (Rd) and outside Beijing (b), averaged concentrations for the sites on the third, fourth and/or fifth ring roads and non-road sites (NRS) (c). One asterisk on bars denotes significant difference at  $p < 0.05$ , while two asterisks on bars denote significant difference at  $p < 0.01$ .

spectively (Fig. 2A, panel a). The average  $\text{NH}_3$  concentrations during the three periods for the sites, inside the sixth ring road (including road sites, or RS, on the third, fourth and fifth ring roads and non-road sites, or NRS), outside the sixth ring road but in Beijing and outside Beijing, are shown in Fig. 2A (panels b and c). The mean  $\text{NH}_3$  concentration inside the sixth ring road was significantly smaller (by 13%) during the Parade Blue period compared with the mean during the post-Parade Blue period ( $20.2 \pm 1.2 \mu\text{g m}^{-3}$  vs.  $23.3 \pm 1.8 \mu\text{g m}^{-3}$ ); further, on all three ring roads reductions (23 to 35%) of the mean during the Parade Blue period were statistically significant while at the non-road sites a small non-significant increase (15%) in the mean was observed (Fig. 2A, panel c). The mean  $\text{NH}_3$  concentration outside the sixth ring road was 12%

smaller in the Parade Blue period than in the post-Parade Blue period ( $21.4 \pm 6.0 \mu\text{g m}^{-3}$  vs.  $24.3 \pm 9.3 \mu\text{g m}^{-3}$ ), whereas outside Beijing, non-significant increases (on average 80%) in the mean occurred during the Parade Blue period ( $26.7 \pm 12.6 \mu\text{g m}^{-3}$ ) compared with those during the pre- and post-Parade Blue periods ( $19.9 \pm 6.2$  and  $11.8 \pm 2.3 \mu\text{g m}^{-3}$ , respectively).

Ambient  $\text{NO}_2$  concentrations ranged from 21.5 to 227.7, 14.1 to 258.8 and 15.7 to 751.8  $\mu\text{g m}^{-3}$  during the pre-Parade Blue, Parade Blue and post-Parade Blue periods, respectively (Fig. 2B, panel a). The mean  $\text{NO}_2$  concentrations at the sites inside the sixth ring road (including road sites on the fifth ring road and NRS), outside the sixth ring road and outside Beijing during the three periods are shown in Fig. 2B (panels b and c). Inside the sixth ring road, the mean

**Table 1.** Mean (standard error) ambient concentrations of PM<sub>2.5</sub> and associated ionic components at the urban and rural sites. PBP denotes the Parade Blue Period.

	Urban site (Site 22) in Beijing			Rural site (Site 29) in Shandong			Rural site (Site 30) in Hebei		
	Pre- PBP ( <i>n</i> = 11)	PBP <sup>a</sup> ( <i>n</i> = 15) <sup>b</sup>	Post- PBP ( <i>n</i> = 15)	Pre- PBP ( <i>n</i> = 6)	PBP ( <i>n</i> = 5)	Post- PBP ( <i>n</i> = 10)	Pre- PBP ( <i>n</i> = 6)	PBP ( <i>n</i> = 5)	Post- PBP ( <i>n</i> = 8)
PM <sub>2.5</sub>	72.37 (7.36)**	37.23 (5.37)	58.49 (7.99)	90.27 (8.53)*	53.84 (11.37)	55.30 (7.45)	38.73 (5.17)	29.44 (6.55)	59.73 (16.35)
NO <sub>3</sub> <sup>-</sup>	2.07 (0.60)	0.85 (0.15)	6.27 (1.72)**	4.21 (1.71)	1.22 (0.22)	5.56 (1.03)**	0.58 (0.22)	1.02 (0.05)	3.46 (0.81)*
SO <sub>4</sub> <sup>2-</sup>	13.26 (2.85)**	3.79 (0.69)	10.92 (2.94)	25.53 (3.36)*	11.55 (3.20)	14.80 (2.84)	9.57 (1.07)*	6.04 (0.65)	8.21 (0.89)
NH <sub>4</sub> <sup>+</sup>	4.62 (0.94)**	1.15 (0.26)	4.07 (1.25)	8.85 (0.91)*	3.49 (1.01)	4.32 (0.98)	2.41 (0.30)**	0.58 (0.18)	2.34 (0.40)**
Ca <sup>2+</sup>	0.58 (0.04)**	0.38 (0.06)	0.51 (0.07)	0.29 (0.06)	0.29 (0.11)	0.23 (0.05)	0.19 (0.07)	0.12 (0.02)	0.09 (0.02)
K <sup>+</sup>	0.30 (0.04)**	0.15 (0.02)	0.42 (0.08)**	0.76 (0.07)	0.50 (0.11)	0.99 (0.18)	0.20 (0.03)	0.18 (0.02)	0.24 (0.02)
F <sup>-</sup>	0.17 (0.02)*	0.10 (0.01)	0.07 (0.02)	0.04 (0.03)	0.07 (0.03)	0.10 (0.04)	0.01 (0.00)	0.00 (0.00)	0.00 (0.00)
Cl <sup>-</sup>	0.11 (0.01)	0.11 (0.01)	0.13 (0.03)	0.14 (0.03)	0.29 (0.14)	0.19 (0.06)	0.06 (0.03)	0.01 (0.00)	0.24 (0.09)*
Na <sup>+</sup>	0.10 (0.02)	0.09 (0.02)	0.25 (0.05)**	0.25 (0.05)	0.45 (0.25)	0.42 (0.04)	0.35 (0.08)	0.52 (0.06)	0.26 (0.02)**
Mg <sup>2+</sup>	0.08 (0.01)**	0.05 (0.01)	0.07 (0.01)	0.05 (0.01)	0.15 (0.12)	0.07 (0.01)	0.03 (0.00)**	0.04 (0.00)	0.04 (0.00)
SIA <sup>c</sup>	19.95 (3.83)**	5.78 (1.00)	21.26 (5.83)*	38.58 (3.75)**	16.26 (4.19)	24.68 (4.61)	12.56 (1.43)*	7.64 (0.81)	14.00 (1.97)*
SIA/PM <sub>2.5</sub> (%)	25.4 (3.2)	20.0 (4.2)	29.0 (4.8)	42.9 (2.3)	31.4 (3.7)	45.6 (4.7)	35.1 (5.2)	30.4 (5.6)	30.1 (4.4)

<sup>a</sup> Parade Blue period. <sup>b</sup> Number of samples. <sup>c</sup> Secondary inorganic aerosol. \* Significant at the 0.05 probability level. \*\* Significant at the 0.01 probability level.

concentration during the Parade Blue period ( $78.7 \mu\text{g m}^{-3}$ ) was 42 and 35 % lower ( $p < 0.01$ ) than the means during the pre- and post-Parade Blue periods ( $135.7 \pm 21.8$  and  $121.0 \pm 16.5 \mu\text{g m}^{-3}$ , respectively). For the fifth ring RS and NRS, most reductions (33–42 %) in the mean during the Parade Blue period were also highly significant ( $p < 0.01$ ). Inside the sixth ring road, a large non-significant reduction (59 %) in the mean concentration occurred during the Parade Blue period compared with the post-Parade Blue period ( $183.5 \pm 49.1$  vs.  $443.4 \pm 173.3 \mu\text{g m}^{-3}$ ). Outside Beijing, the change in the mean during the Parade Blue period ( $23.7 \pm 3.6 \mu\text{g m}^{-3}$ ) was small and non-significant when compared with the means during the pre- and post-Parade periods ( $27.5 \pm 4.5$  and  $18.5 \pm 1.7 \mu\text{g m}^{-3}$ , respectively).

### 3.2 Concentrations of PM<sub>2.5</sub> and its chemical components

A statistical analysis of concentrations of PM<sub>2.5</sub> mass and associated inorganic WSIs at sites 22, 29 and 30 in the three periods is presented in Table 1. Daily PM<sub>2.5</sub> concen-

trations ranged from 4.2 to 123.6, 15.4 to 116.0 and 12.4 to  $170.7 \mu\text{g m}^{-3}$  at sites 22, 29 and 30, respectively. At sites 22 and 29, mean PM<sub>2.5</sub> concentrations during the Parade Blue period decreased significantly (by 49 and 40 %, respectively) compared with the means during the pre-Parade Blue period, and increased again during the post-Parade Blue period (57 and 3 %, respectively) compared with the means during the Parade Blue period. At site 30, a 24 % reduction in mean PM<sub>2.5</sub> concentrations occurred during the Parade Blue period compared with the pre-Parade Blue period and a 103 % increase during the post-Parade Blue period.

Secondary inorganic aerosols (SIA) (sum of NH<sub>4</sub><sup>+</sup>, NO<sub>3</sub><sup>-</sup> and SO<sub>4</sub><sup>2-</sup>) were major components of PM<sub>2.5</sub>, with average contributions of 24, 41 and 32 % to the daily average PM<sub>2.5</sub> mass at sites 22, 29 and 30, respectively. As with PM<sub>2.5</sub> concentrations, concentrations of all the WSIs (except for Cl<sup>-</sup>) at site 22 decreased significantly during the Parade Blue period compared with the pre- and/or post-Parade Blue periods. Analogous behaviour also occurred at sites 29 and 30

for concentrations of  $\text{NO}_3^-$ ,  $\text{NH}_4^+$  and  $\text{SO}_4^{2-}$  but not for those of most of other ions (e.g.  $\text{Ca}^{2+}$ ,  $\text{K}^+$ ,  $\text{F}^-$ ,  $\text{Na}^+$ ).

### 3.3 Daily mean pollutant concentrations from MEP

Daily mean concentrations of the five major pollutants ( $\text{PM}_{2.5}$ ,  $\text{PM}_{10}$ ,  $\text{NO}_2$ ,  $\text{SO}_2$  and  $\text{CO}$ ) at 291 cities in China, divided into three groups of Beijing, cities in emission control regions (excluding Beijing) and cities in non-emission control regions, are summarized in Fig. 3. Average concentrations of  $\text{PM}_{2.5}$ ,  $\text{PM}_{10}$ ,  $\text{NO}_2$ ,  $\text{SO}_2$  and  $\text{CO}$  during the Parade Blue period were highly significantly ( $p < 0.01$ ) decreased in Beijing, with reductions of 72, 67, 39, 34 and 39 %, respectively, compared with the pre-Parade Blue period.  $\text{PM}_{2.5}$  concentrations in Beijing, for example, remained below  $20 \mu\text{g m}^{-3}$  for 14 consecutive days in the Parade Blue period (for comparison, the WHO and China's (first-grade) thresholds for daily  $\text{PM}_{2.5}$  concentrations are 25 and  $35 \mu\text{g m}^{-3}$ , respectively). The daily  $\text{PM}_{2.5}$  concentrations in Beijing in the pre-Parade Blue period averaged  $59 \mu\text{g m}^{-3}$ . Concentrations of  $\text{PM}_{2.5}$ ,  $\text{PM}_{10}$  and  $\text{SO}_2$  in the Parade Blue period were also significantly ( $p < 0.05$ ) decreased in cities in emission control regions (excluding Beijing), with reductions of 32, 29 and 7 %, respectively, while concentrations of  $\text{NO}_2$  and  $\text{CO}$  did not show statistically significant changes ( $p > 0.05$ ). After the Parade Blue period, concentrations of the five major pollutants in Beijing and surrounding regions rebounded quickly, with significant increases of 50–214 and 16–44 %, respectively. In cities in other regions, by contrast, where no additional emission reduction measures were taken, concentrations of  $\text{PM}_{2.5}$ ,  $\text{PM}_{10}$ ,  $\text{NO}_2$ ,  $\text{SO}_2$  and  $\text{CO}$  remained stable or were significantly ( $p < 0.05$ ) higher during the Parade Blue period compared with the pre- and post-Parade Blue periods.

## 4 Discussion

### 4.1 Effect of emission controls on air quality

The statistical analyses (Fig. 3) show that, by taking regional emission controls during the Parade Blue period, daily concentrations of the five reported pollutants ( $\text{PM}_{2.5}$ ,  $\text{PM}_{10}$ ,  $\text{NO}_2$ ,  $\text{SO}_2$  and  $\text{CO}$ ) in Beijing and surrounding other cities in the six provinces were decreased by various but statistically significant amounts, in sharp contrast to increases in cities in other parts of China where no additional emission controls were imposed. This shows the effectiveness of the pollution controls and suggests that air quality improvement was directly related to the reduction intensities of pollutant emissions (e.g. air pollution control effects ranked by Beijing (largest reduction) > emission control regions surrounding Beijing (moderate reduction) > other regions (no reduction) in China). Another way of quantifying the effect of the additional control measures for Beijing uses the Air Quality Index (MEPC, 2012). On the basis of the calculated AQI

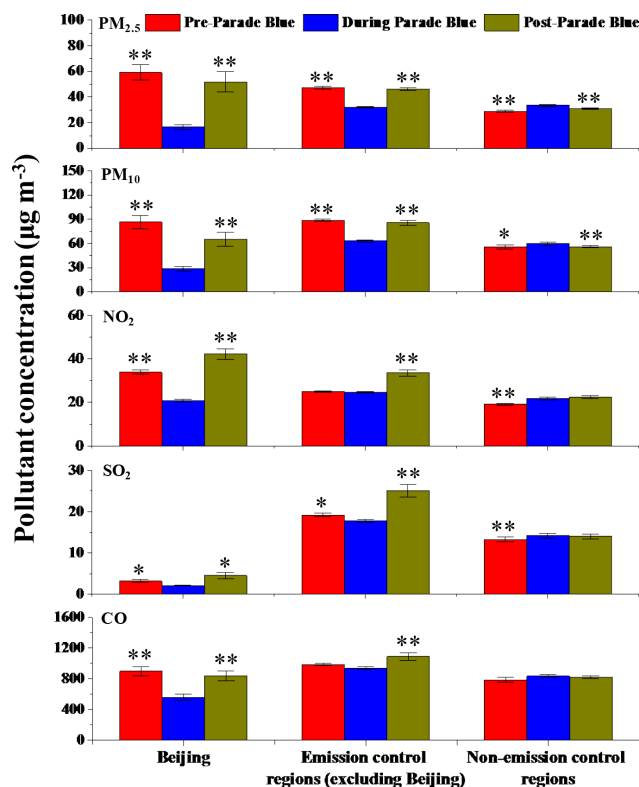


**Figure 3.** Comparison of  $\text{PM}_{2.5}$ ,  $\text{PM}_{10}$ ,  $\text{NO}_2$ ,  $\text{SO}_2$  and  $\text{CO}$  concentrations between non-Parade Blue periods (the pre- and post-Parade Blue periods) and Parade Blue period at Beijing, cities in emission control regions (excluding Beijing) and other cities in non-emission control regions (one asterisk on bars denotes significant difference at  $p < 0.05$ , while two asterisks on bars denote significant difference at  $p < 0.01$ ).

(Fig. 4), defined “good” and polluted days (i.e. “slightly polluted” and “moderately polluted”) altogether accounted for 89 % during the pre-Parade Blue period and 70 % during the post-Parade Blue period. The primary pollutant was  $\text{PM}_{2.5}$  for 82 and 63 % of these days during the pre- and post-Parade Blue periods, respectively. In contrast, almost all of the days during the Parade Blue period were defined as “excellent”. Thus improved air quality, as represented by the AQI during the Parade Blue period, was mainly attributed to the additional control of  $\text{PM}_{2.5}$  precursors.

Results from the MEP of source apportionment of  $\text{PM}_{2.5}$  for Beijing ([http://www.bj.xinhuanet.com/bjyw/2014-04/17/c\\_1110289403.htm](http://www.bj.xinhuanet.com/bjyw/2014-04/17/c_1110289403.htm)) showed that 64–72 % of atmospheric  $\text{PM}_{2.5}$  during 2012–2013 was generated by emissions from local sources, of which the biggest contributor was vehicle exhaust (31.1 %), followed by coal combustion (22.4 %), industrial production (18.1 %), soil dust (14.3 %) and others (14.1 %). The contribution from vehicles had increased by 1.7 percentage points compared to 2010–2011. To examine the contribution of vehicles, power plants and industries to  $\text{PM}_{2.5}$  concentrations,  $\text{PM}_{2.5}$  concentrations from these were

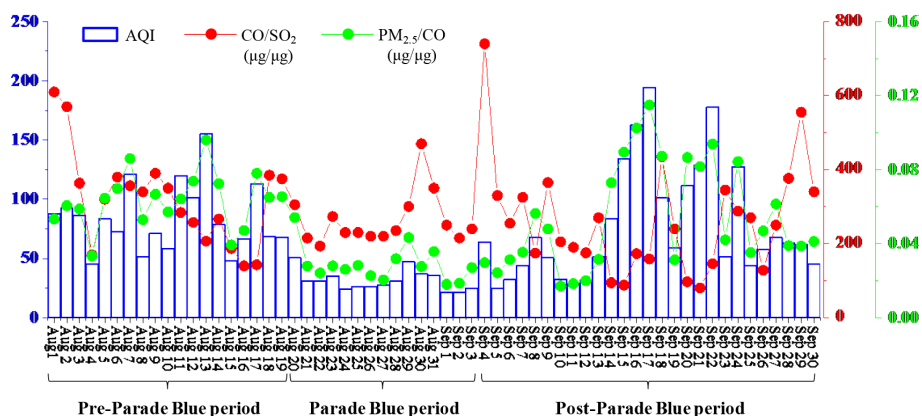


**Figure 4.** Daily values of AQI and daily ratios of CO to SO<sub>2</sub> concentrations and of PM<sub>2.5</sub> to CO concentrations in Beijing during the pre-Parade Blue, Parade Blue and post-Parade Blue periods.

compared with those of other primary pollutants such as NO<sub>x</sub> (NO + NO<sub>2</sub>), CO and SO<sub>2</sub> (Zhao et al., 2012). As shown in Fig. S2a–d, the linear correlations of PM<sub>2.5</sub> with each pollutant gas (CO, NO<sub>2</sub> and SO<sub>2</sub>) and their sum were positive and highly significant ( $R = 0.40\text{--}0.88$ ,  $p < 0.05$ ) during the study period, except for the relationship between PM<sub>2.5</sub> and NO<sub>2</sub> during the pre-Parade Blue period and that of PM<sub>2.5</sub> vs. SO<sub>2</sub> during the Parade Blue period, both of which were positive but not significant ( $p > 0.05$ ). This finding is consistent with the source apportionment results that suggest traffic, power plants and industry are significant sources of PM<sub>2.5</sub> in Beijing. Given the importance of local vehicle emissions vs. more distant power plant and industrial emissions for Beijing's air quality, the ratio of CO/SO<sub>2</sub> can be used as an indicator of the contribution of local emissions to air pollution, with higher ratios indicating higher local contributions (Tang et al., 2015). Ratios of CO/SO<sub>2</sub> decreased (on average by 18 %) from the pre-Parade Blue to Parade Blue period and then increased abruptly on 4 September in the Post-Parade Blue period (Fig. 4), further suggesting the decreased amount of pollutants from local contributions. Beijing has relatively little industry but numerous automobiles, and the emissions of SO<sub>2</sub> are small while those of CO and NO<sub>x</sub> are much larger (Zhao et al., 2012). Thus, traffic emission is likely to be a determining factor influencing urban CO and NO<sub>x</sub> levels. This, in combination with a strong positive and highly significant correlation of PM<sub>2.5</sub> versus CO + NO<sub>2</sub> during the study period (Fig. S2e) and the weak correlation of PM<sub>2.5</sub> vs. SO<sub>2</sub> noted above (Fig. S2c), shows that traffic emission controls should be a priority in mitigating PM<sub>2.5</sub> pollution in the future.

Concentrations of PM<sub>2.5</sub> levels in Beijing are not only driven by primary emissions but are also affected by meteorology and atmospheric chemistry operating on the primary pollutants, leading to secondary pollutant formation (Zhang et al., 2015). To quantify the likely contribution of secondary pollutant formation of PM<sub>2.5</sub> as a contributor to

the observed changes between the Parade Blue period and pre- and post-measurements, CO provides an excellent tracer for primary combustion sources (de Gouw et al., 2009). Daily ratios of PM<sub>2.5</sub>/CO during the Parade Blue period decreased significantly on average by 50 and 40 % relative to the pre- and post-Parade Blue periods, respectively (Fig. 4), which suggests that the significant reduction of PM<sub>2.5</sub> concentrations during the Parade Blue period was not only due to less anthropogenic primary emissions but also due to reduced secondary pollutant formation. This is further supported by our measured results at urban site 22, where average SIA concentrations comprised 20–29 % of average PM<sub>2.5</sub> mass over the three periods and decreased significantly during the Parade Blue period compared with those during the pre- and post-Parade Blue periods (Table 1). Significant reduction of concentrations of precursor gases (e.g. NO<sub>2</sub>, SO<sub>2</sub> and NH<sub>3</sub>) at the city scale is likely to be the major reason for such reduced secondary pollutant formation. In addition, lower concentrations of sulfate and nitrate during the Parade Blue period might also be caused by lower oxidation rates of SO<sub>2</sub> and NO<sub>x</sub>. The sulfur oxidation ratio ( $\text{SOR} = n\text{SO}_4^{2-} / (n\text{SO}_4^{2-} + n\text{SO}_2)$ ) and the nitrogen oxidation ratio ( $\text{NOR} = n\text{NO}_3^- / (n\text{NO}_3^- + n\text{NO}_2)$ ) ( $n$  refers to the molar concentration) are indicators of secondary pollutant transformation in the atmosphere. Higher values of SOR and NOR imply more complete oxidation of gaseous species to sulfate- and nitrate-containing secondary particles (Sun et al., 2006). To understand the potential change in the degree of oxidation of sulfur and nitrogen, we used daily concentrations of SO<sub>4</sub><sup>2-</sup> and NO<sub>3</sub><sup>-</sup> measured at urban site 22 (located at west campus of China Agricultural University) and the MEP-reported concentrations of SO<sub>2</sub> and NO<sub>2</sub> at the Wanliu monitoring station to calculate the SOR and NOR values. This is because these two sites, only 7 km apart (Fig. S3), experience similar pollution climates. The average values of SOR and NOR were 0.64 and 0.04 during the pre-Parade Blue period, 0.47 and 0.03 during the Parade Blue period



and 0.48 and 0.07 during the Post-Parade Blue period, respectively (Fig. S4). Compared with the pre- and post-Parade Blue periods, slightly reduced values of SOR and NOR during the Parade Blue period suggest a possible minor role for changes in the extent of photochemical oxidation in secondary transformation.

Ammonia is the primary alkaline trace gas in the atmosphere. In ammonia-rich environments,  $\text{NH}_4\text{HSO}_4$  and  $(\text{NH}_4)_2\text{SO}_4$  are sequentially formed, and the surplus  $\text{NH}_3$  that does not react with  $\text{H}_2\text{SO}_4$  can form  $\text{NH}_4\text{NO}_3$  (Wang et al., 2005). In both the pre-Parade Blue and Parade Blue periods,  $\text{NH}_4^+$  was strongly correlated with  $\text{SO}_4^{2-}$  (Fig. S5a and c) and  $[\text{SO}_4^{2-} + \text{NO}_3^-]$  (Fig. S5b and d), and the regression slopes were both 0.87 during the pre-Parade Blue period, 0.97 and 0.91 during the Parade Blue period and 1.13 and 0.79 during the post-Parade Blue period, respectively. These results indicate almost complete neutralization of acidic species ( $\text{HNO}_3$  and  $\text{H}_2\text{SO}_4$ ) by  $\text{NH}_3$  in  $\text{PM}_{2.5}$  during these three periods especially in the Parade Blue period. In this way, SIA concentrations from these sources could not be further reduced during the Parade Blue period unless  $\text{NH}_3$  emissions were reduced more than those of  $\text{SO}_2$  and  $\text{NO}_x$ .

#### 4.2 Impact of traffic $\text{NH}_3$ emission on urban $\text{NH}_3$ concentration

The sources of  $\text{NH}_3$  are often dominated by agriculture, but it may also be produced by motor vehicles due to the over-reduction of NO in catalytic converters (Kean and Harley, 2000). The contribution of traffic to the total  $\text{NH}_3$  emissions is estimated at approximately 2% in Europe (EEA, 2011) and 5% in the US (Kean et al., 2009). In China,  $\text{NH}_3$  emissions from traffic rose from 0.005 Tg (contributing approximately 0.08% to total  $\text{NH}_3$  emissions) in 1980 to 0.5 Tg (contributing approximately 5% to total emissions) in 2012 (Kang et al., 2016). Recent studies have discussed the origin of atmospheric  $\text{NH}_3$  in Beijing based on the  $\delta^{15}\text{N}$  technique (Chang et al., 2016; Pan et al., 2016). For example, Chang et al. (2016) identified that non-agricultural sources, merged with waste and traffic  $\text{NH}_3$  emissions, collectively accounted for approximately 50% of ambient  $\text{NH}_3$  in urban Beijing before and after APEC summit, of which more than 20% was sourced from traffic emissions. Traffic is therefore likely to make a very significant contribution to  $\text{NH}_3$  concentrations in urban areas of Beijing, and a strong correlation of  $\text{NH}_3$  with traffic-related pollutants was observed ( $\text{NO}_x$  and CO) at the urban sites (Ianniello et al., 2010; Meng et al., 2011). However, this relationship has a large uncertainty because the concentrations of pollutants used to establish the relationship were measured at “background” urban sites some distance from major roads, and other urban sources such as decaying organic matter may contribute. In the present study, strong and significant correlations were observed between  $\text{NH}_3$  and  $\text{NO}_2$  concentrations measured on the fifth ring road during all three periods (Fig. 5). In addition, compared with

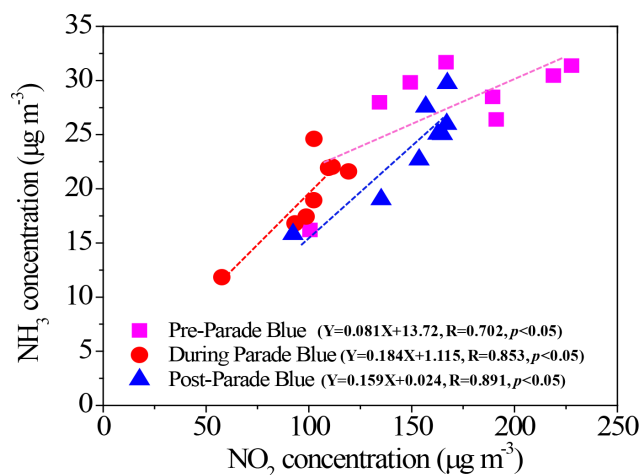


**Figure 5.** Correlations between  $\text{NO}_2$  and  $\text{NH}_3$  concentrations measured on the fifth ring road in Beijing during the pre-Parade Blue, Parade Blue and post-Parade Blue periods.

the averages for the three ring roads during the pre- and/or post-Parade Blue periods, the average  $\text{NH}_3$  concentrations during the Parade Blue period decreased significantly due to traffic reduction measures (Fig. 2A, panel c). These results provide strong evidence that traffic is an important source of  $\text{NH}_3$  in Beijing. In addition to period-to-period temporal changes, the mean  $\text{NH}_3$  concentration at all road sites was 1.3 and 1.9 times that at all non-road sites during the Parade Blue period and post-Parade Blue period, respectively (Fig. 2A). Moreover, during the post-Parade Blue period the measured  $\text{NH}_3$  concentrations on the three ring roads ( $28.3 \pm 6.4 \mu\text{g m}^{-3}$ ) were twice those at the rural sites 29 and 30 ( $14.0 \pm 1.6 \mu\text{g m}^{-3}$ ) affected by intense agricultural  $\text{NH}_3$  emissions. These results, along with the fact that urban Beijing has a higher relative on-road vehicle density and almost no agricultural activity, suggest that  $\text{NH}_3$  emission and transport from local traffic were the main contributors to high urban  $\text{NH}_3$  concentrations. Based on a mileage-based  $\text{NH}_3$  emission factors of  $28 \pm 5$  (assumed as the lower limit; Chang et al., 2016) and  $230 \pm 14.1 \text{ mg km}^{-1}$  (assumed as the upper limit; Liu et al., 2014) for light-duty gasoline vehicles, a population of 5.61 million vehicles (average mileage  $21\,849 \text{ km vehicle}^{-1} \text{ yr}^{-1}$ ) in Beijing would produce approximately 3.4–28 kt  $\text{NH}_3$  in 2015, which likely declined by up to 4.7–38 t  $\text{NH}_3 \text{ day}^{-1}$  during the Parade Blue period given that the traffic load decreased by half with the implementation of the odd-and-even car ban policy. For accurately determining  $\text{NH}_3$  emissions, however, further study of  $\text{NH}_3$  emission factors for vehicles and other sources is warranted.

#### 4.3 Impact of meteorological conditions and long-range air transport

Meteorological conditions strongly regulate near-surface air pollutant concentrations (Liu et al., 2015), contributing the

largest uncertainties to the evaluation of the effects of emission controls on pollutant reduction. Here we first compared the meteorological data obtained during the Parade Blue period with those from the pre- and/or post-Parade Blue periods in Beijing and other cities over northern China. In Beijing, neither WS nor RH differed significantly between non-Parade Blue (the pre- and post-Parade Blue) and the Parade Blue periods, while temperature ( $T$ ) showed a significant but small decrease with time (Fig. 6). Similarly, there were small and non-significant changes in  $T$ , WS and RH between the pre-Parade Blue and Parade Blue periods for emission control regions (excluding Beijing) and for non-emission-control regions in China. These results suggest that the period-to-period changes in  $T$ , WS and RH may have only a minor impact on  $\text{PM}_{2.5}$ ,  $\text{PM}_{10}$ ,  $\text{NO}_2$ ,  $\text{SO}_2$  and CO concentrations in the emission control regions (Fig. 3). In contrast, a higher temperature during the Parade Blue period, compared to the post-Parade Blue period, can in part explain the corresponding higher  $\text{NH}_3$  concentrations measured at NRS due to increased  $\text{NH}_3$  emissions from biological sources such as humans, sewage systems and organic waste in garbage containers (Reche et al., 2012).

Surface weather maps of China (Fig. S6) and northern China (Fig. 7) showed an apparent change of wind field over Beijing and its surrounding regions during the Parade Blue period compared with the other two periods. As shown in Fig. 7, Beijing was located at the rear of a high-pressure system within the southeast–south flow or in a high-pressure area when the wind was weak ( $< 3 \text{ m s}^{-1}$ ) and at the base of the Siberian high-pressure system when influenced by a weak cold front and easterly wind ( $> 4 \text{ m s}^{-1}$ ) in the non-Parade (pre- or post-Parade) Blue and Parade Blue periods, respectively. The former weather condition (non-Parade Blue periods) was conducive to pollutant convergence and the latter (Parade Blue period) was conducive to pollutant dispersion. A further analysis of wind rose plots (Fig. 8a) showed that northerly winds, with similar wind speeds, dominated all three periods. Northerly–northwesterly winds in Beijing bring relatively clean air due to a lack of heavy industry in the areas north–northwest of Beijing. Winds during the pre- and post-Parade Blue periods were occasionally from the south, southeast and east of Beijing, where the regions (e.g. Hebei, Henan and Shandong provinces) are characterized by substantially higher anthropogenic emissions of air pollutants such as  $\text{NH}_3$ ,  $\text{NO}_x$ ,  $\text{SO}_2$  and aerosols (Zhang et al., 2009, 2010; Gu et al., 2012). Also as mentioned earlier, the topography of the mountains to the west and north of Beijing effectively traps the polluted air over Beijing during southerly air-flow, suggesting that the southerly wind during non-Parade Blue periods may enhance air pollution in Beijing. Wet scavenging from precipitation, although often important in summer (Yoo et al., 2014), probably played a minor role in changing the concentrations of pollutants given the low and comparable precipitation over Beijing and surrounding areas during the study periods (Fig. 8). For example, the total pre-

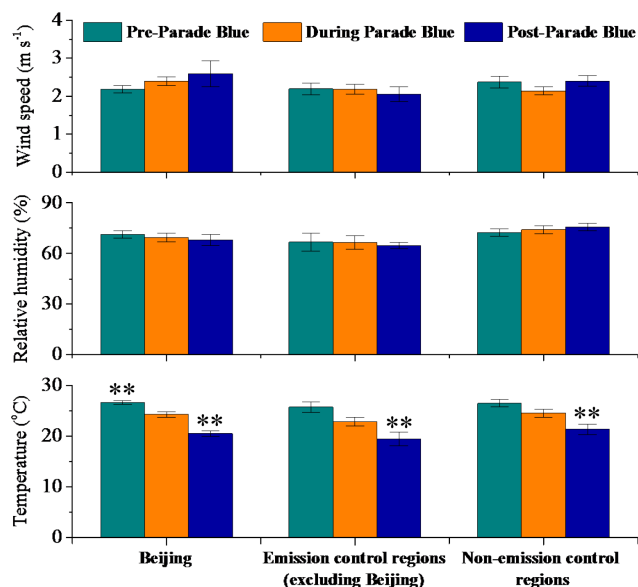


**Figure 6.** Comparison of wind speed (WS), relative humidity (RH) and temperature ( $T$ ) between the Parade Blue period and non-Parade Blue periods (the pre-Parade Blue and post-Parade Blue periods) in Beijing, emission control regions (excluding Beijing) and other cities in non-emission-control regions (two asterisk on bars denotes significant difference at  $p < 0.01$ ).

cipitation in Beijing was comparable between the pre-Parade Blue and Parade Blue periods (38.9 vs. 34.4 mm) (Fig. 8b). In addition, we compared daily mean MLH in Beijing during the study period (Fig. 9a). The daily mean MLH in Beijing was approx. 37% higher during the Parade Blue period (1777 m) than the pre-Parade (1301 m) and post-Parade (1296 m) Blue periods (Fig. 9b,  $p = 0.08$ ). Since the MLH during Parade Blue was higher than that during non-Parade Blue periods, the horizontal and vertical diffusion conditions during the Parade Blue period were better than the other two periods.

Changes in meteorological conditions often lead to changes in regional pollution transport and ventilation. It has been shown that regional transport from neighbouring Tianjin, Hebei, Shanxi and Shandong provinces can have a significant impact on Beijing's air quality (Meng et al., 2011; Zhang et al., 2015). Model calculations by Zhang et al. (2015) suggested that about half of Beijing's  $\text{PM}_{2.5}$  pollution originates from sources outside of the city. Trajectory analysis in previous studies revealed that the air mass from south and southeast regions of Beijing led to high concentrations of  $\text{NH}_3$ ,  $\text{NO}_x$ ,  $\text{PM}_{2.5}$  and secondary inorganic ions during summertime (Ianniello et al., 2010; Wang et al., 2010; Sun et al., 2015). The 72-hour back trajectories during the three measurement periods, shown in Fig. 10, were classified into four sectors according to air mass pathways: the west pathway over southern Mongolia, western Inner Mongolia, and Xinjiang, the north pathway over Inner Mongolia,

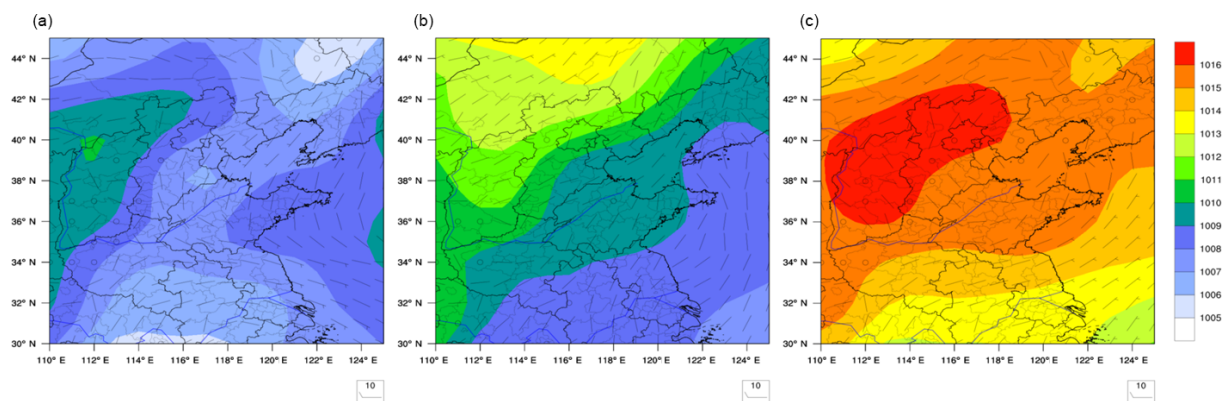


**Figure 7.** Mean sea level pressure (unit: hPa) and mean wind field at 10 m height (unit:  $\text{m s}^{-1}$ ) during the pre-Parade Blue (a), Parade Blue (b) and post-Parade Blue (c) periods in Beijing and northern China. The colour bar denotes air pressure (unit: hPa) and arrows reflect wind vector (unit:  $\text{m s}^{-1}$ ).

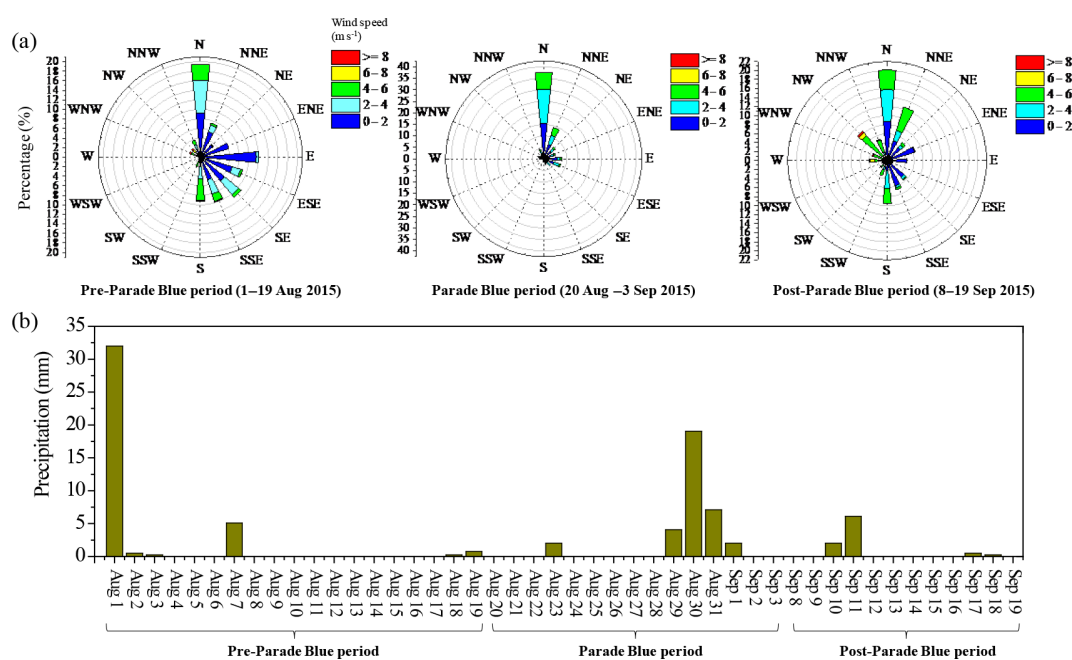


**Figure 8.** The frequency distributions of wind directions and speeds (colour demarcation) (a) and daily precipitation amount (b) in Beijing during the pre-Parade Blue, Parade Blue and post-Parade Blue periods.

Heilongjiang and north Hebei provinces, the east pathway mainly over northeast Hebei province and Tianjin municipality, and the south sector over the south Hebei and Shandong provinces. The results indicated that transport of regional pollution from the south sector occurred during the pre-Parade Blue period (38 %) and the post-Parade Blue period (18 % for  $\text{PM}_{2.5}$  sampling days and 29 % for  $\text{NH}_3$  sampling days) but there was no transport of regional pollution during the Parade Blue period. As the south of Hebei province contains heavily polluting industry and intensive agriculture (Zhang et al., 2009; Sun et al., 2015), the absence of transport of air masses from the south sector is likely at least partly responsible for lower concentrations of the five

reported pollutants ( $\text{PM}_{2.5}$ ,  $\text{PM}_{10}$ ,  $\text{NO}_2$ ,  $\text{SO}_2$  and CO) during the Parade Blue period. As for  $\text{NH}_3$ , however, average concentration at NRS were slightly higher in the Parade Blue period than in the post-Parade Blue period (Fig. 2A, panel c), indicating that surface levels of  $\text{NH}_3$  were less influenced by southern air masses. Much of the airflow travelled over Tianjin municipality during the Parade Blue period (32 %) compared to that during the post-Parade Blue period (19 %) (Fig. 10b and d), which probably caused the high surface  $\text{NH}_3$  concentrations in Beijing. This is because Tianjin, as one of the megacities in China, has high  $\text{NH}_3$  emissions from livestock and fertilizer application (Zhang et al., 2010).

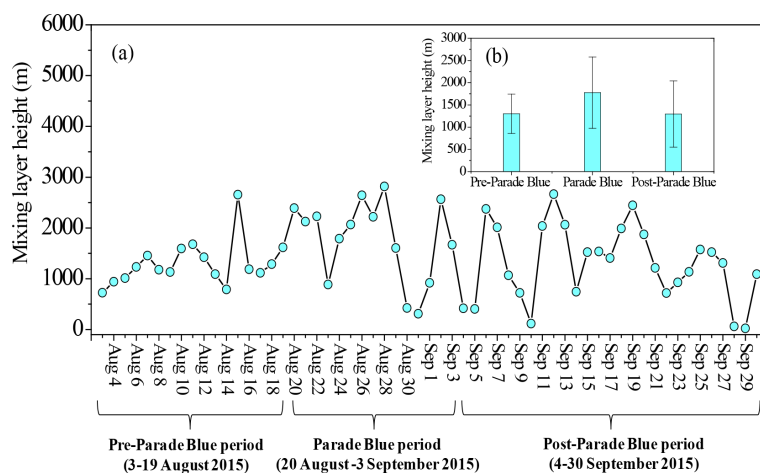


**Figure 9.** Dynamics of daily mean atmospheric mixing layer height (MLH) in Beijing from 3 August to 30 September 2015 (a) and comparison of MLH means during the pre-Parade Blue, Parade Blue and post-Parade Blue periods (b).

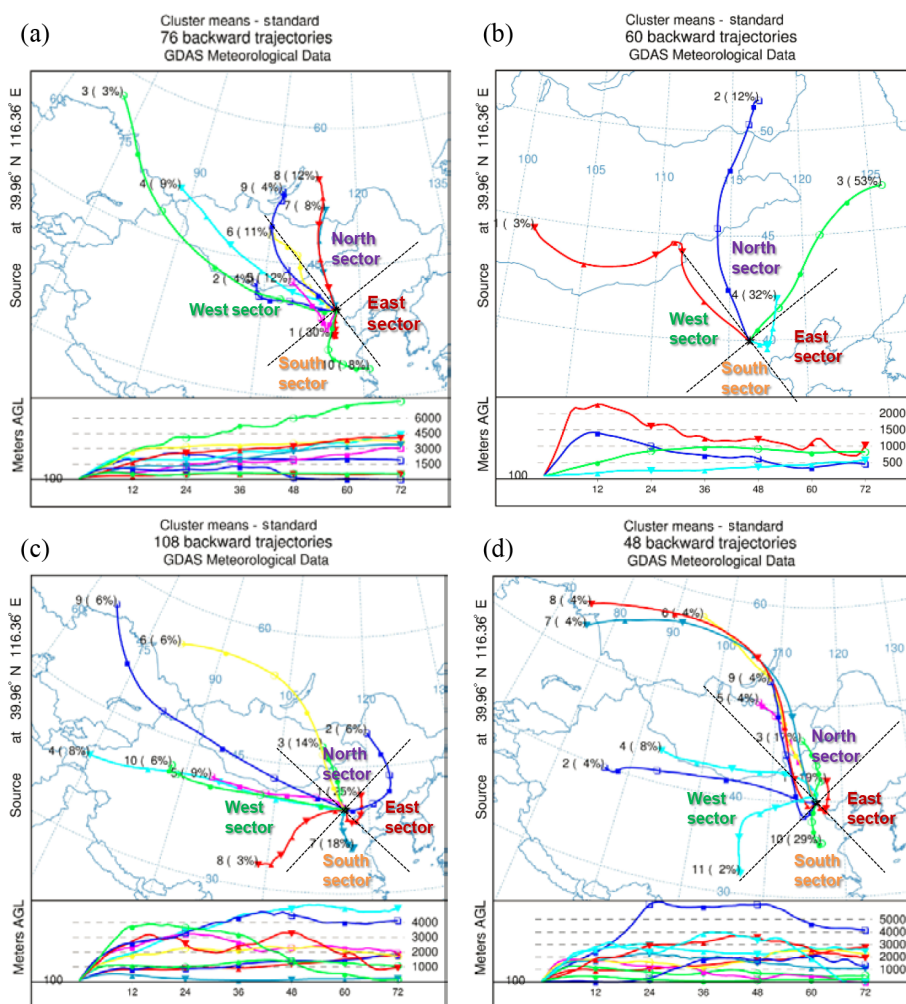


**Figure 10.** Seventy-two-hour backward trajectories for 100 m a.g.l. (above ground level) in Beijing during the pre-Parade Blue period (1 to 19 August 2015) (a), the Parade Blue period (20 August to 3 September 2015) (b), and the post-Parade Blue period (4 to 30 September 2015) (c) and for sampling duration of NH<sub>3</sub> (8 to 19 September 2015) in the post-Parade Blue period (d).

To further diagnose the impacts of meteorology on the surface air quality, we conducted a simulation using the nested GEOS-Chem atmospheric chemistry model driven by the GEOS-FP assimilated meteorological fields at  $1/4^\circ \times 5/16^\circ$  horizontal resolution covering East Asia ( $70\text{--}140^\circ\text{E}$ ,  $15\text{--}55^\circ\text{N}$ ) (Zhang et al., 2015, 2016). Details of the model emissions and mechanisms have been described in Zhang et al. (2016), focusing on  $\text{PM}_{2.5}$  concentrations in Beijing during the Asia-Pacific Economic Cooperation Summit (APEC; 5–11 November) period. We used anthropogenic emissions from the Multi-Resolution Emission Inventory of China for the year 2010 (MEIC, 2015), except for  $\text{NH}_3$  emissions that were taken from the Regional Emission in Asia (REAS-v2) inventory (Kurokawa et al., 2013) with an improved seasonality derived by Zhao et al. (2015).

We conducted a standard simulation with fixed anthropogenic emissions for the period of 1 August–12 September 2015. By fixing anthropogenic emissions in the simulation, the model provides a quantitative estimate of the meteorological impacts alone before and during the Parade Blue period. For the pre-Parade period (1–19 August), the model-simulated mean  $\text{PM}_{2.5}$  concentration is  $62\ \mu\text{g m}^{-3}$  in Beijing, comparable to the measured values ( $59\ \mu\text{g m}^{-3}$ ), but simulated  $\text{NH}_3$  concentrations are too low ( $3\ \mu\text{g m}^{-3}$  vs.  $8.2\text{--}31.7\ \mu\text{g m}^{-3}$ ), probably due to missing urban  $\text{NH}_3$  sources and the coarse model resolution ( $1/4^\circ \times 5/16^\circ$ ). Here we focus on the model simulated relative changes in pollutant concentrations before and during the Parade Blue period. Model results showed that, without emission controls, the air pollutant concentrations in Beijing in the Parade Blue period relative to the pre-Parade period would be 29% lower for  $\text{PM}_{2.5}$ , 7% lower for  $\text{NH}_3$ , 17% lower for  $\text{SO}_2$ , 8% lower for CO and relatively no change for  $\text{NO}_2$  (Fig. 11a) as a result of the different meteorological conditions as discussed above. Thus, compared with meteorological condition changes, air pollution control measures made a greater contribution to air quality improvement (especially for  $\text{PM}_{2.5}$ ,  $\text{NO}_x$  and CO) in Beijing during the Parade Blue period (Fig. 11b).

We also conducted two sensitivity simulations for the Parade Blue period (20 August–3 September) to examine the responses of  $\text{PM}_{2.5}$  concentrations to emission reductions: (1) with anthropogenic emissions of  $\text{NH}_3$  reduced by 40% over Beijing and by 30% over Hebei and Tianjin and (2) with all anthropogenic emissions including  $\text{NH}_3$ ,  $\text{SO}_2$ ,  $\text{NO}_x$ , CO and primary aerosol reduced by 40% over Beijing and by 30% over Hebei and Tianjin. We find that the  $\text{NH}_3$  emission reduction (by 40% over Beijing and by 30% over Hebei and Tianjin) could decrease the mean  $\text{PM}_{2.5}$  concentration in Beijing by 12% for the period, compared with 31% simulated  $\text{PM}_{2.5}$  reduction if all anthropogenic emissions were reduced by the same amount. This supports our findings on the effectiveness of emission controls during the Parade Blue period as indicated in the measurements and the high sensitivity of  $\text{PM}_{2.5}$  concentration in Beijing to  $\text{NH}_3$  sources.

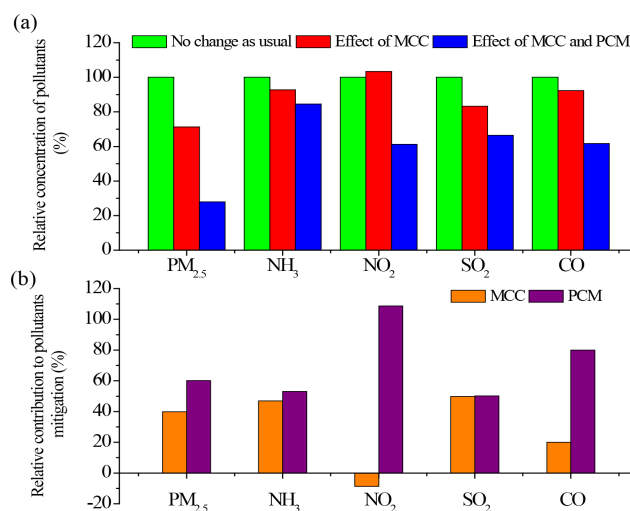


**Figure 11.** Effect of meteorological condition change (MCC, simulated by a GEOS-Chem chemical transport model) and pollution control measures (PCM, measured by monitoring stations) to relative concentrations of CO,  $\text{NO}_2$ ,  $\text{SO}_2$ ,  $\text{NH}_3$  and  $\text{PM}_{2.5}$  (a) and relative contribution of MCC and PCM to major pollutant mitigation (b) in Beijing during the Parade Blue period.

#### 4.4 Implications for regional air pollution control

Besides Tianjin, Beijing is surrounded by four provinces, Hebei, Shandong, Henan and Shanxi, which all have major power plants and manufacturing industry. In the INTEX-B emission inventory, the total emissions from these four provinces accounted for 28.7, 27.9, 28.3 and 25.0% of national emissions of  $\text{PM}_{2.5}$ ,  $\text{PM}_{10}$ ,  $\text{SO}_2$  and  $\text{NO}_x$ , respectively (Zhang et al., 2009). The “Parade Blue” experience demonstrates that, by taking appropriate but strict coordinated regional and local emission controls, air quality in megacities can be significantly and quickly improved.

China is not the first country to use temporal emission control strategies. In 1996, the city of Atlanta, for example, adopted a series of actions to reduce traffic volume and significantly improved air quality during the Atlanta Olympic Games (Tian and Brimblecombe, 2008; Peel et al., 2010). We also should note that most of these emission control strategies have not been maintained after the Olympic Games. In the long term, temporary emission control strategies will not improve regional air quality conditions and we should seek better ways towards sustainable development. Integrated emission reduction measures are therefore necessary, but meteorological conditions also need to be considered for a sustainable solution, as in Urumqi, northwestern China (Song et al., 2015). We therefore recommend further efforts to build on the Parade Blue experience of successful air quality improvement in Beijing and the surrounding region to improve air pollution control policies throughout China and in other rapidly developing countries.

Chinese national SO<sub>2</sub> emissions have been successfully reduced by 14 % from the 2005 level due to an SO<sub>2</sub> control policy (Wang et al., 2014), and nationwide controls on NO<sub>x</sub> emissions have been implemented along with the controls on SO<sub>2</sub> and primary particles during 2011–2015. However, there is as yet no regulation or policy that targets national NH<sub>3</sub> emissions. Future emission control policies to mitigate PM and SIA pollution in China should, in addition to focusing on primary particles NO<sub>x</sub> and SO<sub>2</sub>, also address NH<sub>3</sub> emission reduction from both agricultural and non-agricultural sectors (e.g. traffic sources) in particular when NH<sub>3</sub> becomes key to PM<sub>2.5</sub> formation (Liu et al., 2013; Wu et al., 2016; Xu et al., 2016).

## 5 Conclusions

We have presented atmospheric concentrations of NH<sub>3</sub>, NO<sub>2</sub>, PM<sub>2.5</sub> and associated inorganic water-soluble ions before, during and after the Parade Blue period measured at 31 in situ sites in and outside Beijing, as well as daily concentrations of PM<sub>2.5</sub>, PM<sub>10</sub>, NO<sub>2</sub>, SO<sub>2</sub> and CO in 291 cities in China during the pre-Parade Blue and Parade Blue periods released by the MEP of China. Our unique study examines temporal variations at local and regional scales across China and the relative role of the emission controls and meteorological conditions, as well as the contribution of traffic, to NH<sub>3</sub> levels in Beijing based on the first direct measurements of NH<sub>3</sub> and NO<sub>2</sub> concentrations at road sites. The following major findings and conclusions were reached.

The concentrations of NH<sub>3</sub> and NO<sub>2</sub> during the Parade Blue period at the road sites in different areas of Beijing decreased significantly by 12–35 and 34–59 %, respectively, relative to the pre- and post-Parade Blue measurements, while those at the non-road sites showed an increase of 15 % for NH<sub>3</sub> and reductions of 33 and 42 % for NO<sub>2</sub>. Positive and significant correlations were observed between NH<sub>3</sub> and NO<sub>2</sub> concentrations measured at road sites. Taken together, these findings indicate that on-road traffic is an important source of NH<sub>3</sub> in the urban Beijing. Daily concentrations of PM<sub>2.5</sub> and secondary inorganic aerosols (sulfate, ammonium and nitrate) at the urban and rural sites both decreased during the Parade Blue period, which was closely related to controls of secondary aerosol precursors (NH<sub>3</sub>, SO<sub>2</sub> and NO<sub>x</sub>) and/or reduced secondary pollutant formation.

During the Parade Blue period, daily concentrations of air pollutants (PM<sub>2.5</sub>, PM<sub>10</sub>, NO<sub>2</sub>, SO<sub>2</sub> and CO) in 291 cities obtained from the national air quality monitoring network showed large and significant reductions of 34–72 % in Beijing, small reductions of 1–32 % in emission control regions (excluding Beijing) and slight increases (6–16 %) in non-emission-control regions that in some cases were significant, which reflects the positive effects of emission controls on air quality and suggests that the extent of air quality improve-

ment was directly associated with the reduction intensities of pollutant emissions.

A detailed characterization of meteorological parameters and regional transport demonstrated that the good air quality in Beijing during the Parade Blue period was the combined result of emission controls, meteorological effects and the absence of transport of air masses from the south of Beijing. Thus, the net effectiveness of emission controls was investigated further by excluding the effects of meteorology in model simulations, which showed that emission controls can contribute reductions of pollutant concentrations of nearly 60 % for PM<sub>2.5</sub>, 109 % for NO<sub>2</sub>, 80 % for CO, 53 % for NH<sub>3</sub> and 50 % for SO<sub>2</sub>. This result showed that emission controls played a dominant role in air quality improvement in Beijing during the Parade Blue period.

## 6 Data availability

The data used in this study are available from the corresponding author upon request (liu310@cau.edu.cn).

**The Supplement related to this article is available online at doi:10.5194/acp-17-31-2017-supplement.**

*Author contributions.* Xuejun Liu and Fusuo Zhang designed the research. Xuejun Liu, Wen Xu, Wei Song, Yangyang Zhang, Daowei Yang, Dandan Wang, Zhang Wen and Aohan Tang conducted the research (collected the data and performed the measurements). Wen Xu, Wei Song, Lin Zhang and Xuejun Liu wrote the manuscript. All authors were involved in the discussion and interpretation of the data as well as the revision of the manuscript.

*Acknowledgements.* We thank Lu Li, Hao Tianxiang, Wang Sen and Wang Wei for their assistance during the field measurements. This work was financially supported by the 973 project (2014BC954200) and the National Natural Science Foundation of China (41425007, 31421092).

Edited by: J. Liggio

Reviewed by: three anonymous referees

## References

- Chan, C. K. and Yao, X. H.: Air pollution in mega cities in China, *Atmos. Environ.*, 42, 1–42, doi:10.1016/j.atmosenv.2007.09.003, 2008.
- Chang, Y. H., Liu, X. J., Deng, C. R., Dore, A. J., and Zhuang, G. S.: Source apportionment of atmospheric ammonia before, during, and after the 2014 APEC summit in Beijing using stable nitrogen isotope signatures, *Atmos. Chem. Phys.*, 16, 11635–11647, doi:10.5194/acp-16-11635-2016, 2016.

- Chen, C., Sun, Y. L., Xu, W. Q., Du, W., Zhou, L. B., Han, T. T., Wang, Q. Q., Fu, P. Q., Wang, Z. F., Gao, Z. Q., Zhang, Q., and Worsnop, D. R.: Characteristics and sources of submicron aerosols above the urban canopy (260 m) in Beijing, China, during the 2014 APEC summit, *Atmos. Chem. Phys.*, 15, 12879–12895, doi:10.5194/acp-15-12879-2015, 2015.
- Chen, R. S., De Sherbinin, A., Ye, C., and Shi, G. Q.: China's Soil Pollution: Farms on the Frontline, *Science*, 344, 691–691, 2014.
- Davis, D. L., Bell, M. L., and Fletcher, T.: A Look Back at the London Smog of 1952 and the Half Century Since, *Environ. Health Persp.*, 110, A734–A735, 2002.
- de Gouw, J. A., Welsh-Bon, D., Warneke, C., Kuster, W. C., Alexander, L., Baker, A. K., Beyersdorf, A. J., Blake, D. R., Canagaratna, M., Celada, A. T., Huey, L. G., Junkermann, W., Onasch, T. B., Salcido, A., Sjostedt, S. J., Sullivan, A. P., Tanner, D. J., Vargas, O., Weber, R. J., Worsnop, D. R., Yu, X. Y., and Zaveri, R.: Emission and chemistry of organic carbon in the gas and aerosol phase at a sub-urban site near Mexico City in March 2006 during the MILAGRO study, *Atmos. Chem. Phys.*, 9, 3425–3442, doi:10.5194/acp-9-3425-2009, 2009.
- Draxler, R. R. and Hess, G.: Description of the HYSPLIT4 modeling system, Air Resources Laboratory, Silver Spring, Maryland, 1997.
- Draxler, R., Stunder, B., Rolph, G., Stein, A., and Taylor, A.: HYSPLIT4 user's guide, version 4, report, NOAA, Silver Spring, MD, 2012.
- EEA – European Environment Agency: Air Quality in Europe – 2011 Report, Technical Report 12/2011, EEA, Copenhagen, 2011.
- Gu, B. J., Ge, Y., Ren, Y., Xu, B., Luo, W. D., Jiang, H., Gu, B. H., and Chang, J.: Atmospheric reactive nitrogen in China: Sources, recent trends, and damage costs, *Environ. Sci. Technol.*, 46, 9240–9247, doi:10.1021/es301446g, 2012.
- Guo, J. H., Liu, X. J., Zhang, Y., Shen, J. L., Han, W. X., Zhang, W. F., Christie, P., Goulding, K., Vitousek, P., and Zhang, F. S.: Significant soil acidification in major Chinese croplands, *Science*, 327, 1008–1010, doi:10.1126/science.1182570, 2010.
- Haagen-Smit, A. J.: Chemistry and physiology of Los Angeles smog, *Ind. Eng. Chem.*, 44, 1342–1346, doi:10.1021/ie50510a045, 1952.
- Holzworth, G. C.: Estimates of mean maximum mixing depths in the contiguous United States, *Mon. Weather Rev.*, 92, 235–242, 1964.
- Holzworth, G. C.: Mixing depths, wind speeds and air pollution potential for selected locations in the United States, *J. Appl. Meteorol.*, 6, 1039–1044, 1967.
- Huang, R.-J., Zhang, Y., Bozzetti, C., Ho, K.-F., Cao, J.-J., Han, Y., Daellenbach, K. R., Slowik, J. G., Platt, S. M., Canonaco, F., Zotter, P., Wolf, R., Pieber, S. M., Brun, E. A., Crippa, M., Ciarelli, G., Piazzalunga, A., Schwikowski, M., Abbaszade, G., Schnelle-Kreis, J., Zimmermann, R., An, Z., Szidat, S., Baltensperger, U., Haddad, I. E., and Prevot, A. S. H.: High secondary aerosol contribution to particulate pollution during haze events in China, *Nature*, 514, 218–222, 2014.
- Ianniello, A., Spataro, F., Esposito, G., Allegrini, I., Rantica, E., Ancora, M. P., Hu, M., and Zhu, T.: Occurrence of gas phase ammonia in the area of Beijing (China), *Atmos. Chem. Phys.*, 10, 9487–9503, doi:10.5194/acp-10-9487-2010, 2010.
- Kang, Y. N., Liu, M. X., Song, Y., Huang, X., Yao, H., Cai, X. H., Zhang, H. S., Kang, L., Liu, X. J., Yan, X. Y., He, H., Zhang, Q., Shao, M., and Zhu, T.: High-resolution ammonia emissions inventories in China from 1980 to 2012, *Atmos. Chem. Phys.*, 16, 2043–2058, doi:10.5194/acp-16-2043-2016, 2016.
- Kean, A. J. and Harley, R. A.: On-road measurement of ammonia and other motor vehicle exhaust emissions, *Environ. Sci. Technol.*, 34, 3535–3539, doi:10.1021/es991451q, 2000.
- Kean, A. J., Littlejohn, D., Ban-Weiss, G. A., Harley, R. A., Kirchstetter, T. W., and Lunden, M. M.: Trends in on-road vehicle emissions of ammonia, *Atmos. Environ.*, 43, 1565–1570, doi:10.1016/j.atmosenv.2008.09.085, 2009.
- Liu, T. Y., Wang, X. M., Wang, B. G., Ding, X., Deng, W., Lu, S. J., and Zhang, Y. L.: Emission factor of ammonia (NH<sub>3</sub>) from on-road vehicles in China: tunnel tests in urban Guangzhou, *Environ. Res. Lett.*, 9, 064027, doi:10.1088/1748-9326/9/6/064027, 2014.
- Liu, X. J., Zhang, Y., Han, W. X., Tang, A. H., Shen, J. L., Cui, Z. L., Vitousek, P., Erismann, J. W., Goulding, K., Christie, P., Fangmeier, A., and Zhang, F. S.: Enhanced nitrogen deposition over China, *Nature*, 494, 459–462, doi:10.1038/nature11917, 2013.
- Liu, Z. R., Hu, B., Wang, L. L., Wu, F. K., Gao, W. K., and Wang, Y. S.: Seasonal and diurnal variation in particulate matter (PM<sub>10</sub> and PM<sub>2.5</sub>) at an urban site of Beijing: analyses from a 9-year study, *Environ. Sci. Pollut. Res.*, 22, 627–642, doi:10.1007/s11356-014-3347-0, 2015.
- Lu, Y. L., Song, S., Wang, R. S., Liu, Z. Y., Meng, J., Sweetman, A. J., Jenkins, A., Ferrier, R. C., Li, H., Luo, W., and Wang, T. Y.: Impacts of soil and water pollution on food safety and health risks in China, *Environ. Int.*, 77, 5–15, doi:10.1016/j.envint.2014.12.010, 2015.
- MEIC – Multi-Resolution Emission Inventory of China for the year 2010: available at: <http://meicmodel.org>, last access: 1 February 2015.
- Meng, Z. Y., Lin, W. L., Jiang, X. M., Yan, P., Wang, Y., Zhang, Y. M., Jia, X. F., and Yu, X. L.: Characteristics of atmospheric ammonia over Beijing, China, *Atmos. Chem. Phys.*, 11, 6139–6151, doi:10.5194/acp-11-6139-2011, 2011.
- MEPC – Ministry of Environmental Protection of China: Ambient air quality standards (GB3095-2012), available at: <http://www.mep.gov.cn/>, last access: 29 February 2012.
- Pan, Y. P., Tian, S. L., Liu, D. W., Fang, Y. T., Zhu, X. Y., Zhang, Q., Zheng, B., Michalski, G., and Wang, Y. S.: Fossil fuel combustion-related emissions dominate atmospheric ammonia sources during severe haze episodes: evidence from <sup>15</sup>N stable isotope in size-resolved aerosol ammonium, *Environ. Sci. Technol.*, 50, 8049–8056, doi:10.1021/acs.est.6b00634, 2016.
- Parrish, D. D., Singh, H. B., Molina, L., and Madronich, S.: Air quality progress in North American megacities: a review, *Atmos. Environ.*, 45, 7015–7025, doi:10.1016/j.atmosenv.2011.09.039, 2011.
- Peel, J. L., Klein, M., Flanders, W. D., Mulholland, J. A., Tolbert, P. E., and Committee, H. H. R.: Impact of improved air quality during the 1996 summer Olympic games in Atlanta on multiple cardiovascular and respiratory outcomes, Research Report 148, 3–23, discussion 25–33, Health Effect Institute, USA, 2010.
- Reche, C., Viana, M., Pandolfi, M., Alastuey, A., Moreno, T., Amato, F., Ripoll, A., and Querol, X.: Urban NH<sub>3</sub> levels and sources

- in a Mediterranean environment, *Atmos. Environ.*, 57, 153–164, doi:10.1016/j.atmosenv.2012.04.021, 2012.
- Shen, J. L., Tang, A. H., Liu, X. J., Kopsch, J., Fangmeier, A., Goulding, K., and Zhang, F. S.: Impacts of pollution controls on air Quality in Beijing during the 2008 Olympic Games, *J. Environ. Qual.*, 40, 37–45, doi:10.2134/jeq2010.0360, 2011.
- Song, W., Chang, Y. H., Liu, X. J., Li, K. H., Gong, Y. M., He, G. X., Wang, X. L., Christie, P., Zheng, M., Dore, A. J., and Tian, C. Y.: A multiyear assessment of air quality benefits from China's emerging shale gas revolution: Urumqi as a case study, *Environ. Sci. Technol.*, 49, 2066–2072, doi:10.1021/es5050024, 2015.
- Sun, Y. L., Zhuang, G. S., Tang, A. H., Wang, Y., and An, Z. H.: Chemical Characteristics of PM<sub>2.5</sub> and PM<sub>10</sub> in haze-fog episodes in Beijing, *Environ. Sci. Technol.*, 40, 3148–3155, doi:10.1021/es051533g, 2006.
- Sun, Y. L., Wang, Z. F., Du, W., Zhang, Q., Wang, Q. Q., Fu, P. Q., Pan, X. L., Li, J., Jayne, J., and Worsnop, D. R.: Long-term real-time measurements of aerosol particle composition in Beijing, China: seasonal variations, meteorological effects, and source analysis, *Atmos. Chem. Phys.*, 15, 10149–10165, doi:10.5194/acp-15-10149-2015, 2015.
- Tang, G., Zhu, X., Hu, B., Xin, J., Wang, L., Munkel, C., Mao, G., and Wang, Y.: Impact of emission controls on air quality in Beijing during APEC 2014: lidar ceilometer observations, *Atmos. Chem. Phys.*, 15, 12667–12680, doi:10.5194/acp-15-12667-2015, 2015.
- Tao, Y., Yin, Z., Ye, X. N., Ma, Z., and Che, J. M.: Size distribution of water-soluble inorganic ions in urban aerosols in Shanghai, *Atmos. Pollut. Res.*, 5, 639–647, doi:10.5094/APR.2014.073, 2014.
- Tian, Q. W., and Brimblecombe, P.: Managing air in Olympic cities, *Am. J. Environ. Sci.*, 4, 439–444, 2008.
- Wang, S. X., Xing, J., Zhao, B., Jang, C., and Hao, J. M.: Effectiveness of national air pollution control policies on the air quality in metropolitan areas of China, *J. Environ. Sci.*, 26, 13–22, doi:10.1016/S1001-0742(13)60381-2, 2014.
- Wang, T., Nie, W., Gao, J., Xue, L. K., Gao, X. M., Wang, X. F., Qiu, J., Poon, C. N., Meinardi, S., Blake, D., Wang, S. L., Ding, A. J., Chai, F. H., Zhang, Q. Z., and Wang, W. X.: Air quality during the 2008 Beijing Olympics: secondary pollutants and regional impact, *Atmos. Chem. Phys.*, 10, 7603–7615, doi:10.5194/acp-10-7603-2010, 2010.
- Wang, W. T., Primbs, T., Tao, S., and Simonich, S. L. M.: Atmospheric Particulate Matter Pollution during the 2008 Beijing Olympics, *Environ. Sci. Technol.*, 43, 5314–5320, 2009.
- Wang, Y., Zhuang, G., Tang, A., Yuan, H., Sun, Y., Chen, S., and Zheng, A.: The ion chemistry of PM<sub>2.5</sub> aerosol in Beijing, *Atmos. Environ.*, 39, 3771–3784, doi:10.1016/j.atmosenv.2005.03.013, 2005.
- Wu, Y., Gu, B., Erisman, J. W., Reis, S., Fang, Y., Lu, X., and Zhang, X.: PM<sub>2.5</sub> pollution is substantially affected by ammonia emissions in China, *Environ. Pollut.*, 218, 86–94, doi:10.1016/j.envpol.2016.08.027, 2016.
- Xu, W., Zheng, K., Liu, X. J., Meng, L. M., Huaitalla, M. R., Shen, J. L., Hartung, E., Gallmann, E., Roelcke, M., and Zhang, F. S.: Atmospheric NH<sub>3</sub> dynamics at a typical pig farm in China and their implications, *Atmos. Pollut. Res.*, 5, 455–463, doi:10.5094/APR.2014.053, 2014.
- Xu, W., Luo, X. S., Pan, Y. P., Zhang, L., Tang, A. H., Shen, J. L., Zhang, Y., Li, K. H., Wu, Q. H., Yang, D. W., Zhang, Y. Y., Xue, J., Li, W. Q., Li, Q. Q., Tang, L., Lu, S. H., Liang, T., Tong, Y. A., Liu, P., Zhang, Q., Xiong, Z. Q., Shi, X. J., Wu, L. H., Shi, W. Q., Tian, K., Zhong, X. H., Shi, K., Tang, Q. Y., Zhang, L. J., Huang, J. L., He, C. E., Kuang, F. H., Zhu, B., Liu, H., Jin, X., Xin, Y. J., Shi, X. K., Du, E. Z., Dore, A. J., Tang, S., Collett, J. L., Goulding, K., Sun, Y. X., Ren, J., Zhang, F. S., and Liu, X. J.: Quantifying atmospheric nitrogen deposition through a nationwide monitoring network across China, *Atmos. Chem. Phys.*, 15, 12345–12360, doi:10.5194/acp-15-12345-2015, 2015.
- Xu, W., Wu, Q. H., Liu, X. J., Tang, A. H., Dore, A. J., and Heal, M. R.: Characteristics of ammonia, acid gases, and PM<sub>2.5</sub> for three typical land-use types in the North China Plain, *Environ. Sci. Pollut. Res.*, 23, 1158–1172, doi:10.1007/s11356-015-5648-3, 2016.
- Yoo, J. M., Lee, Y. R., Kim, D., Jeong, M. J., Stockwell, W. R., Kundu, P. K., Oh, S. M., Shin, D. B., and Lee, S. J.: New indices for wet scavenging of air pollutants (O<sub>3</sub>, CO, NO<sub>2</sub>, SO<sub>2</sub>, and PM<sub>10</sub>) by summertime rain, *Atmos. Environ.*, 82, 226–237, doi:10.1016/j.atmosenv.2013.10.022, 2014.
- Zhang, L., Liu, L. C., Zhao, Y. H., Gong, S. L., Zhang, X. Y., Henze, D. K., Capps, S. L., Fu, T. M., Zhang, Q., and Wang, Y. X.: Source attribution of particulate matter pollution over North China with the adjoint method, *Environ. Res. Lett.*, 10, 084011, doi:10.1088/1748-9326/10/8/084011, 2015.
- Zhang, L., Shao, J. Y., Lu, X., Zhao, Y. H., Hu, Y. Y., Henze, D. K., Liao, H., Gong, S. L., and Zhang, Q.: Sources and processes affecting fine particulate matter pollution over North China: an adjoint analysis of the Beijing APEC period, *Environ. Sci. Technol.*, 50, 8731–8740, 2016.
- Zhang, Q., Streets, D. G., Carmichael, G. R., He, K. B., Huo, H., Kannari, A., Klimont, Z., Park, I. S., Reddy, S., Fu, J. S., Chen, D., Duan, L., Lei, Y., Wang, L. T., and Yao, Z. L.: Asian emissions in 2006 for the NASA INTEX-B mission, *Atmos. Chem. Phys.*, 9, 5131–5153, doi:10.5194/acp-9-5131-2009, 2009.
- Zhang, T., Cao, J. J., Tie, X. X., Shen, Z. X., Liu, S. X., Ding, H., Han, Y. M., Wang, G. H., Ho, K. F., Qiang, J., and Li, W. T.: Water-soluble ions in atmospheric aerosols measured in Xi'an, China: seasonal variations and sources, *Atmos. Res.*, 102, 110–119, doi:10.1016/j.atmosres.2011.06.014, 2011.
- Zhang, Y., Dore, A. J., Ma, L., Liu, X. J., Ma, W. Q., Cape, J. N., and Zhang, F. S.: Agricultural ammonia emissions inventory and spatial distribution in the North China Plain, *Environ. Pollut.*, 158, 490–501, doi:10.1016/j.envpol.2009.08.033, 2010.
- Zhang, Y. L. and Cao, F.: Fine particulate matter (PM<sub>2.5</sub>) in China at a city level, *Sci. Rep.*, 5, 14884, doi:10.1038/srep14884, 2015.
- Zhao, B., Wang, P., Ma, J. Z., Zhu, S., Pozzer, A., and Li, W.: A high-resolution emission inventory of primary pollutants for the Huabei region, China, *Atmos. Chem. Phys.*, 12, 481–501, doi:10.5194/acp-12-481-2012, 2012.